Higher-order Balmer line indices in α/Fe-enhanced stellar population models

Daniel Thomas, Claudia Maraston, & Andreas Korn
Max-Planck-Institut für extraterrestrische Physik, Giessenbachstraße, D-85748 Garching, Germany

ABSTRACT

We have computed the higher-order Balmer absorption line indices Hγ and Hδ (Worthey & Ottaviani 1997) for stellar population models with variable element ratios. The response of these indices to abundance ratio variations is taken from detailed line formation and model atmosphere calculations. We find that Hγ and Hδ, unlike Hβ, are very sensitive to α/Fe ratio changes at super-solar metallicities. Both line indices increase significantly with increasing α/Fe ratio. This effect cannot be neglected when these line indices are used to derive the ages of metal-rich, unresolved stellar populations like early-type galaxies. We re-analyze the elliptical galaxy sample of Kuntschner (2000), and show that consistent age estimates from Hβ and Hγ are obtained, only if the effect of α/Fe enhancement on Hγ is taken into account in the models. This result rectifies a problem currently present in the literature, namely that Hγ and Hδ have up to now led to significantly younger ages for early-type galaxies than Hβ. Our work particularly impacts on the interpretation of intermediate to high-redshift data, for which only the higher-order Balmer lines are accessible observationally.

Key words: stars: abundances – Galaxy: abundances – globular clusters: general – galaxies: stellar content – galaxies: elliptical and lenticular, cD

1 INTRODUCTION

Absorption line indices in the visual as defined by the Lick group (e.g., Hβ, Mg$_2$, Fe5270, Fe5335, etc., Burstein et al. 1984; Faber et al. 1985) have proven to be a useful tool for the derivation of ages and metallicities of unresolved stellar populations. One of the largest merits of the Lick indices is to have signaled the presence of non-solar Mg/Fe abundance ratios in the stars of early-type galaxies (Worthey, Faber & González 1992; Davies, Sadler & Peletier 1993; Carollo & Danziger 1994; Fisher, Franx & Illingworth 1995; Surma & Bender 1995; Weiss, Peletier & Matteucci 1995; Greggio 1997). This interpretation is confirmed empirically by the similarity between the Lick indices of early-type galaxies and those of Bulge globular clusters (Maraston et al. 2003), which are known from spectroscopy of individual stars to be Mg/Fe enhanced.

Indeed the indices Mg$_2$/Mg b and Fe5270/Fe5335 are dominated by absorption lines from the elements Mg and Fe, and model atmosphere calculations by Barbuy (1994) and Tripicco & Bell (1995) have theoretically demonstrated that these indices are sensitive to Mg/Fe abundance ratios. Following an extension of the method introduced by Trager et al. (2000a), we have used the calculations of Tripicco & Bell (1995) to produce stellar population models with variable element abundance ratios (Thomas, Maraston & Bender 2003a, hereafter TMB03). These models are now able to match simultaneously the Mg and Fe line indices of globular clusters and early-type galaxies.

The Balmer line index Hβ, which is used as age indicator be-

cause it measures the presence of warm A-type stars, is only moderately contaminated by metallic lines and therefore relatively insensitive to abundance ratio variations (Tripicco & Bell 1995; Trager et al. 2000a, TMB03). Does this convenient attribute of Hβ apply also to the higher-order Balmer line indices Hγ and Hδ defined in Worthey & Ottaviani (1997)? The comparison of the predictions from solar-scaled stellar population models with galactic globular cluster data shows that the effect from α/Fe-enhancement must be small in a metallicity range up to solar (Maraston et al. 2003). There are several good reasons for serious doubts, however, that this is the case also at super-solar metallicities. 1) From data in the literature (Kuntschner & Davies 1998; Terlevich et al. 1999; Poggianti et al. 2001; Kuntschner et al. 2002; Trager, Faber & Dressler 2004) it can be seen that the higher-order Balmer line indices and Hβ lead to very inconsistent age estimates. 2) The Hδ measurements of early-type galaxies in the Sloan Digital Sky Survey cannot be reproduced by current solar-scaled stellar population models (Eisenstein et al. 2003). 3) Both Hγ and Hδ have very prominent Fe absorption features in their pseudo-continua.

Tripicco & Bell (1995) have not included Hγ and Hδ, however, so that a quantitative assessment of the sensitivity of these line indices to abundance ratios in stellar population models was not possible until now. Since these line indices are already being widely used and will certainly supersede Hβ as age indicators in future studies at intermediate and high-redshifts, it is urgent to clarify this issue. To this aim in Korn et al. (in preparation) we have extended the Tripicco & Bell (1995) approach and computed model

atmosphere calculations with variable abundance ratios including the wavelengths of the higher-order Balmer lines ($\lambda \sim 4000$ Å). In this paper we present the resulting stellar population models of Hγ and Hδ with different α/Fe ratios, which are computed following the recipe of TMB03.

The paper is organised as follows. In Section 2 we will briefly introduce the stellar population model, and calibrate it with galactic globular clusters. In Section 3 we shall confront the new models with data of elliptical galaxies focusing on the issues outlined above. We will conclude with Section 4.

2   THE MODEL

TMB03 present stellar population models with different chemical mixtures and element abundance ratios. All optical Lick indices from CN$_1$ to TiO$_2$ (Worthey et al. 1994) in the wavelength range 4000 Å $\lesssim \lambda \lesssim 6500$ Å are computed for various chemical mixtures modifying the abundance ratios between α-elements (e.g., O, Mg, Si, Ti etc.), iron peak elements (Fe, Cr), and the individual elements carbon, nitrogen, and calcium (Thomas, Maraston & Bender 2003b). The models are based on the evolutionary population synthesis of Maraston (1998, 2004). The impact from element ratio changes is computed with the help of the Tripicco & Bell (1995) model atmosphere calculations, using an extension of the method introduced by Trager et al. (2000a). We refer to TMB03 for more details.

2.1   New model atmosphere calculations

We have performed model atmosphere calculations based on the code MAFAGS (Gehren 1975a,b) in a large range of metallicities from 1/200 to 3.5 times solar, as presented and described in detail in Korn et al. (in preparation). In the work of Tripicco & Bell (1995), recently defined absorption line indices like the higher-order Balmer lines (Worthey & Ottaviani 1997) or the Ca II triplet (Cenarro et al. 2001) are not included. Our new model atmosphere and line formation calculations allow us to explore abundance ratio effects on any index definition. Here we very briefly summarize the main results found for the higher-order Balmer line indices Hγ and Hδ, relevant for this paper.

We first calculated model atmospheres with solar-scaled element ratios for various combinations of temperature, gravity, and total metallicity. In subsequent models we double in turn the abundances of the elements C, N, O, Mg, Fe, Ca, Na, Si, Cr, and Ti. We find that higher-order Balmer line indices, unlike Hβ, are sensitive to element abundance variations. More specifically, all four indices, Hγ_A, Hγ_F, Hδ_A, and Hδ_F, show significant positive responses to the elements Mg and Si, and significant negative responses to Fe, C, and Ti. The latter are caused by the presence of absorption lines in the pseudo-continua of the absorption index. These sensitivities increase with total metallicity because of the increasing strengths of the metallic lines, and virtually disappear at low metallicities.

2.2   Inclusion in the stellar population model

In the TMB03 models, the α/Fe-enhanced chemical mix at fixed total metallicity is obtained by balancing the increased abundance of the enhanced group with a decrease of the abundances of the elements Fe and Cr (see also Trager et al. 2000a). The former contains the so-called α-elements O, Ne, Mg, Si, S, Ar, Ca, Ti (particles that are build up with α-particle nuclei) plus the elements N and Na. The

abundance of C (formally also an α-particle) is assumed not to vary (see TMB03 for more details). As the enhanced group dominates by far the total metal abundance (mostly because O is the most abundant metal), an enhancement of the α/Fe ratio at fixed total metallicity is characterized mainly by a decrease in the abundances of Fe and Cr. Hence, even though relative variations of the element abundances within the enhanced group exist in early-type galaxies (Worthey 1998; Saglia et al. 2002; Sanchez-Blazquez et al. 2003; Thomas et al. 2003b), these do not significantly affect the α/Fe ratio. This implies that the negative responses of the higher-order Balmer line indices to Fe abundance as reported above will dominate the behaviour of the indices as a function of the α/Fe ratio. A split of the abundance vectors into further components exceeds the scope of this paper and will be subject of future work.

The resulting stellar population models are shown in Fig. 1, in which we plot the α/Fe-independent index $[\mathrm{MgFe}]'$ (see TMB03) vs. Hγ_A, Hγ_F, Hδ_A, and Hδ_F as functions of total metallicity, for the abundance ratios $[\alpha/\mathrm{Fe}] = 0.0$, 0.3, 0.5 (see lables), and a fixed age of 12 Gyr. At high metallicities, the models show a very prominent dependence of all four higher-order Balmer line indices on the α/Fe ratio. This α/Fe-sensitivity disappears at low metallicities, because of the general weakness of Fe and other metal absorption lines.

The effect at high metallicity amounts to the order of a couple of Angstroms. It is caused by the presence of a large number of iron lines, the strongest being Fe I lines at 4308 Å in the blue and at 4383 and 4405 Å in the red pseudo-continua. The most prominent Fe I lines in the index definitions of Hδ_A and Hδ_F are at 4045 Å (only Hδ_A), 4064 and 4072 Å in the blue pseudo-continuum. The red pseudo-continuum of the narrower index Hδ_F contains Fe I lines at 4119 and 4132 Å, the red pseudo-continuum of Hδ_A includes the lines at 4132 and 4144 Å. Hγ seems generally slightly less affected, as this index has Fe and Cr lines at 4326 and 4352 within the absorption feature, which may counter-balance the effect from the iron lines in the continuum windows.

In case of both Hγ and Hδ, the narrower index definitions are less sensitive to abundance ratio variations. It is obvious that the narrower the definition of an index, the less it is affected by contamination from additional metallic lines. There is a price to pay, however. Narrower indices require significantly higher signal-to-noise ratios (Vazdekis & Arimoto 1999), which becomes very expensive in terms of telescope time, and seriously hinders their use for galaxies at intermediate and high redshifts.

2.3   Check with globular clusters

The solar-scaled stellar population models of the higher-order Balmer line indices are presented and compared with globular cluster data in Maraston et al. (2003). Because of their weak sensitivity to α/Fe ratios at metallicities below solar (see Section 2.2), the solar-scaled models reproduce very well the data of globular clusters up to solar metallicity (for the comparison at young ages see Beasley, Hoyle & Sharples 2002). Here we check whether also the new models, with the effect of α/Fe-enhancement included, are consistent with the globular cluster data. In Fig. 1, which is analogous to Fig. 13 in Maraston et al. (2003), globular clusters (Puzia et al. 2002) are plotted as circles. It is known from high-resolution spectroscopy of individual stars in galactic globular clusters that these are α/Fe-enhanced by typically a factor 2 (see Maraston et al. 2003 and references therein). The model can therefore be considered well calibrated, at least for old ages, if the data are reproduced by the model with $[\alpha/\mathrm{Fe}] = 0.3$.
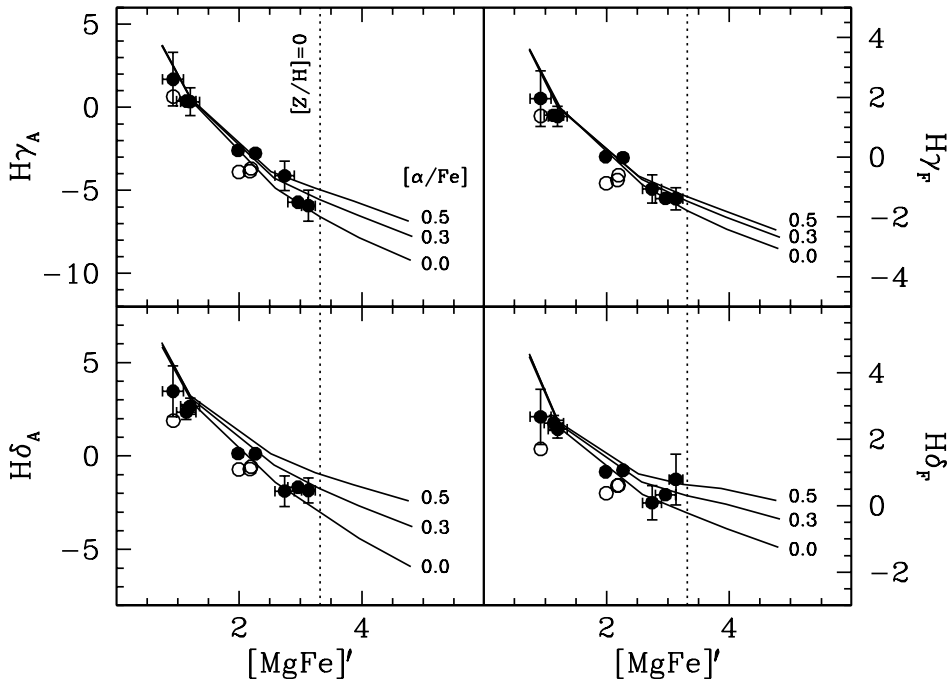
Figure 1. The α/Fe-independent index $[\mathrm{MgFe}]'$ vs. $\mathrm{H}\gamma_\mathrm{A}$, $\mathrm{H}\gamma_\mathrm{F}$, $\mathrm{H}\delta_\mathrm{A}$, and $\mathrm{H}\delta_\mathrm{F}$ as functions of total metallicity, for the abundance ratios $[\alpha/\mathrm{Fe}] = 0.0$, 0.3, 0.5 (see lables), and a fixed age of 12 Gyr. The vertical dotted line indicates the $[\mathrm{MgFe}]'$ of the solar metallicity model. Circles are the indices measured on the integrated light of galactic globular clusters (Puzia et al. 2002). Open circles are globular clusters with horizontal branches that are relatively red given their metallicity (see Maraston et al. 2003).

The proper modelling of Balmer line indices requires the calibration of the horizontal branch morphology (de Freitas Pacheco & Barbuy 1995; Maraston & Thomas 2000; Lee, Yoon & Lee 2000; Maraston et al. 2003). In Maraston et al. (2003) various morphologies of the horizontal branch in the models are considered, that reproduce the data with their observed horizontal branches. Since this issue is fully discussed there, in Fig. 1 we plot only the model which best reproduces the average trend of the Balmer line indices as a function of metallicity. The open symbols are clusters that have relatively red horizontal branches for their metallicity, and it is shown in Maraston et al. (2003) that these objects are well matched by models in which less mass loss along the red giant branch is adopted. Our model predictions should therefore be compared with the filled data points. Hence, the models can be considered well calibrated.

To conclude, as the sensitivity of $\mathrm{H}\gamma$ and $\mathrm{H}\delta$ to α/Fe disappears at low metallicities and is still relatively small around solar metallicity, both the solar-scaled and the α/Fe-enhanced models are consistent with the globular cluster data.

3 THE AGES OF ELLIPTICAL GALAXIES

The effect of the α/Fe ratio on the higher-order Balmer line indices increases significantly with metallicity (Fig. 1), so that a noticeable impact is to be expected on the derivation of ages for metal-rich systems like elliptical galaxies. This is illustrated in Fig. 2, in which we plot the Balmer line indices $\mathrm{H}\gamma_\mathrm{A}$, $\mathrm{H}\gamma_\mathrm{F}$, and $\mathrm{H}\beta$ of elliptical galaxies from the Fornax cluster (Kuntschner 2000) versus their $[\mathrm{MgFe}]'$ indices. Overlayed are solar-scaled (dotted lines) and α/Fe-enhanced (solid lines) model grids for ages from 3 to 15 Gyr and total metallicities $[Z/\mathrm{H}]$ between -0.33 and 0.67 (see

labels). It should be emphasized that the elliptical galaxy data of Kuntschner (2000) are particularly appropriate for the purpose of this paper, as the sample displays an amazingly small spread in α/Fe ratio (see Fig. 2 and text below). This allows us to show only one α/Fe-enhanced model grid, which considerably eases the illustration of the effect of the α/Fe ratio on the age determination.

3.1 Based on solar-scaled models

When interpreted with the solar-scaled models, the three Balmer line indices yield dramatically discrepant age estimates: $\mathrm{H}\gamma_\mathrm{A}$, $\mathrm{H}\gamma_\mathrm{F}$, and $\mathrm{H}\beta$ indicate average ages for the Fornax ellipticals of about 3, 8, and 10 Gyr, respectively. In line with the different ages, also inconsistent metallicities are obtained from the various Balmer lines, $\mathrm{H}\gamma_\mathrm{A}$ leading to the highest values. NGC 1399 (see label) is not even covered by the solar-scaled models for $\mathrm{H}\gamma_\mathrm{A}$ and $\mathrm{H}\gamma_\mathrm{F}$ implying metallicities well above $[Z/\mathrm{H}] = 0.67$ in extrapolation.

3.2 Based on α/Fe-enhanced models

However, from their Mg and Fe indices, we know that the Kuntschner (2000) ellipticals are all α/Fe-enhanced with $[\alpha/\mathrm{Fe}] \sim 0.2$ on the average as shown in the bottom right-hand panel of Fig. 2 (only NGC 1399 has a slightly higher α/Fe). Hence, the appropriate model to be used is the α/Fe-enhanced model with $[\alpha/\mathrm{Fe}] \sim 0.2$ shown as solid lines in Fig. 2. These models predict substantially larger (up to 1 Å) $\mathrm{H}\gamma_\mathrm{A}$, still significantly larger $\mathrm{H}\gamma_\mathrm{F}$, and only moderately larger $\mathrm{H}\beta$ indices than the solar-scaled ones. As a consequence, the severe age discrepancies obtained on the basis of the solar-scaled model are eliminated. When interpreted with the α/Fe-enhanced model, the age and metallicity estimates from
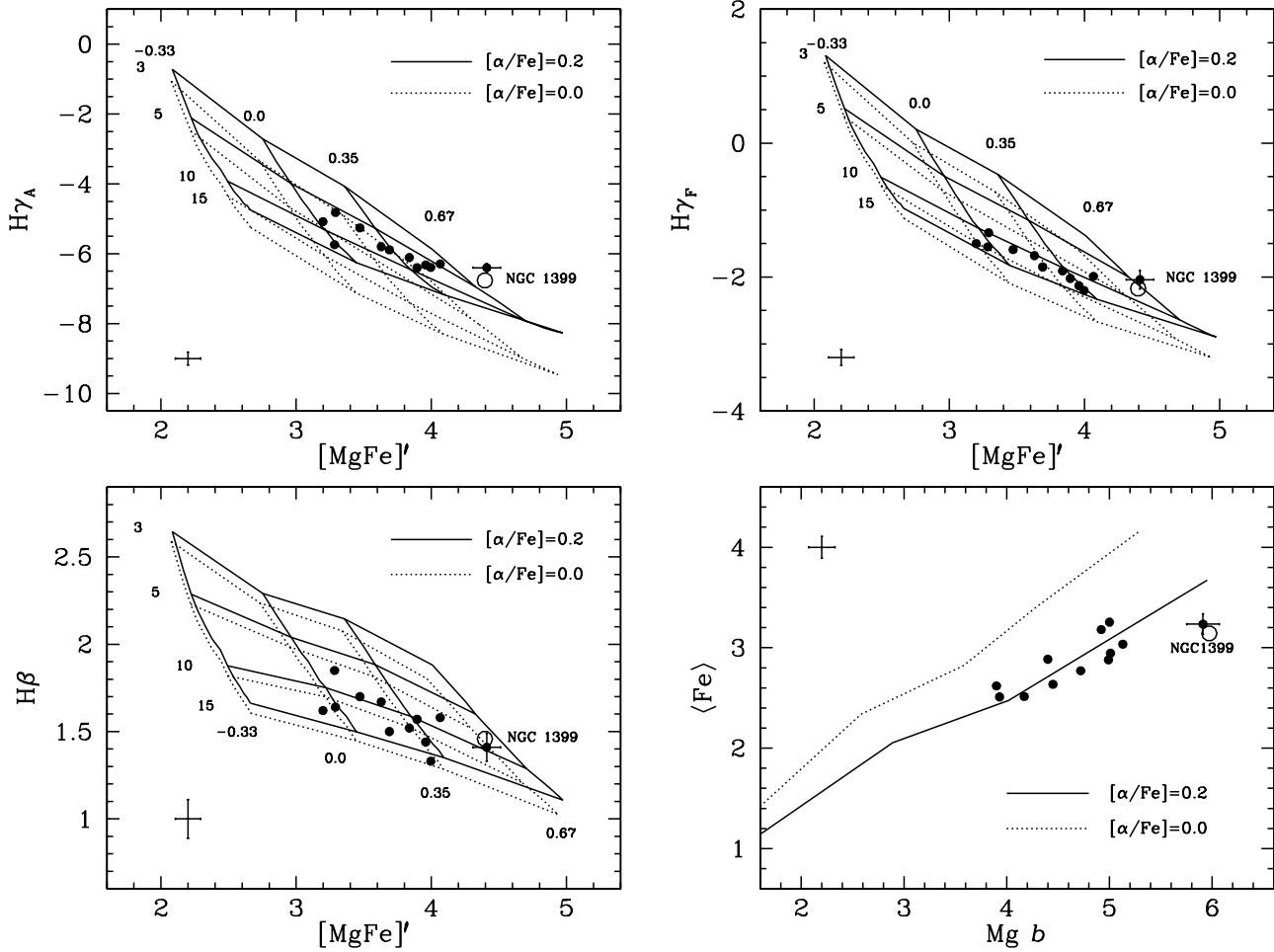
Figure 2. Balmer line indices $H\gamma_A$ (top left-hand panel), $H\gamma_F$ (top right-hand panel) and $H\beta$ (bottom left-hand panel) as functions of the α/Fe-independent index $[MgFe]'$. The bottom right-hand panel shows $Mg\,b$ vs. $\langle Fe \rangle$. Solid and dotted lines are the α/Fe-enhanced and the solar-scales models, respectively. Models for the ages 3, 5, 10, and 15 Gyr (only 10 Gyr in the bottom right-hand panel), and the metallicities $[Z/H] = -0.33$, 0.0, 0.35, 0.67 are shown (see labels). Filled circles are elliptical galaxy data from Kuntschner (2000). The open circle is a model with $t = 9.5$ Gyr, $[Z/H] = 0.58$ and $[\alpha/Fe] = 0.38$ meant to reproduce NGC 1399. The error bars denote average 1-σ errors.

$H\beta$ and $H\gamma_F$ now agree amazingly well. We find the ages to scatter between 10 and 15 Gyr with metallicities between one and two times solar. The same good agreement holds also for NGC 1399. To demonstrate this, we plot as the open circle in Fig. 2 the model prediction with the three parameters $t = 9.5$ Gyr, $[Z/H] = 0.58$ and $[\alpha/Fe] = 0.38$, which reproduces well (within the errors) all six absorption line indices.

The agreement with $H\gamma_A$ is less compelling, even though the situation has clearly improved with respect to the solar-scaled model. The age estimates are roughly consistent within the errors, but we still obtain systematically younger ages from $H\gamma_A$ than from $H\beta$ and $H\gamma_F$. This might be due to an underestimation of the index responses drawn from our model atmosphere calculations (Korn et al., in preparation). However, it cannot be excluded that the fitting functions for $H\gamma_A$ are in error at metallicities above solar owing to bad input stellar data, or that calibration offsets are present in the galaxy data. The former caution can expect clarification, when in future index response functions of the higher-order Balmer lines from other groups will be available (Houdashelt et al. 2002; Trager et al. 2004). To conclude, at this point it is certainly safer to use the narrower definition $H\gamma_F$, if the cost in signal-to-noise is bearable.

3.3 Age determinations in the literature

The content of this paper strongly impacts on some results reported in the literature, which have been obtained by using higher-order Balmer line indices as age indicators. In the previous sections, we have extensively discussed the interpretation of the Kuntschner (2000) sample. A further example is the work by Terlevich et al. (1999), who analyze the $H\gamma_A$ and $H\delta_A$ indices of a sample of ~ 100 Coma galaxies. Interpreting the data with solar-scaled stellar population models, they find relatively young ages for early-type cluster galaxies between 3 and 5 Gyr, and in particular they find the trend that more luminous objects tend to be younger. However, a well-defined correlation between α/Fe-enhancement and galaxy mass is found for early-type galaxies (Trager et al. 2000b; Thomas, Maraston & Bender 2002; Mehlert et al. 2003). Hence, both the young ages and the anti-correlation between age and galaxy luminosity disappear, when the effect from α/Fe ratios on the higher-order Balmer line indices is taken into account.

As a further example, Eisenstein et al. (2003) have recently measured absorption line indices of early-type spectra from the Sloan Digital Sky Survey. They find severe inconsistencies between several line indices. Both $H\beta$ and $Mg\,b$ cannot be matched simul-

taneously with the higher-order Balmer line index $H\delta_A$ by solar-scaled stellar population models for any age-metallicity combination. This problem is caused, at least partially, by abundance ratios effects and can be resolved with the models presented in this paper. We have shown that $H\delta_A$ increases by several Angstroms when the α/Fe ratio is doubled. Note that a more quantitative comparison is not possible, because the data presented in Eisenstein et al. (2003) are not strictly calibrated on the Lick system.

It has also been noticed in the literature that early-type galaxy data are better matched by the solar-scaled models, when higher-order Balmer line indices are plotted as functions of Fe indices (Fe4383, Fe5270) instead (e.g., Kuntschner 2000; Poggianti et al. 2001; Eisenstein et al. 2003). From the models presented here we know now that this apparent consistency between data and models is merely the consequence of two compensating effects: The increase of the higher-order Balmer line indices owing to the α/Fe enhancement is balanced by a decrease of the Fe line indices, which conspires to locate the data on the model grid.

4 CONCLUSIONS

We have extended our models of absorption line indices of stellar populations with variable abundance ratios (TMB03) to the higher-order Balmer line indices $H\gamma_A$, $H\gamma_F$, $H\delta_A$, and $H\delta_F$. We show that the model predictions are well consistent with data of galactic globular clusters. The key result of this work is that, unlike $H\beta$, all four indices show a marked dependence on the α/Fe ratio. The significance of this effect increases with increasing metallicity, and therefore impacts on the age derivation for elliptical galaxies. Re-analyzing the elliptical galaxy sample of Kuntschner (2000), we show that $H\beta$ and $H\gamma_F$ (and a bit less convincingly also $H\gamma_A$) yield consistent age estimates if (and only if) the effect of α/Fe enhancement is taken into account.

A posteriori, it is not surprising that blue absorption line indices are more affected by abundance ratio effects, because of the presence of more metallic lines in the bluer parts of the spectrum. This fact certainly diminishes the advantage of the higher-order Balmer line indices over $H\beta$ as age indicators, in spite of their lower sensitivity to emission line filling. The consequence for the age derivation by means of $H\gamma$ and $H\delta$ is twofold: 1) The element ratio effect on the Balmer line indices needs to be taken into account in the models. 2) The additional knowledge of the α/Fe ratio is necessary, which requires the simultaneous measurement of $Mg\,b$ and Fe5270/Fe5335. If these wavelengths are not accessible, as typically the case for intermediate and high-redshift data, α/Fe ratios may be best estimated from the indices Fe4383 and CN_1 or CN_2.

Model tables are listed in the Appendix and are available electronically under http://www.mpe.mpg.de/∼dthomas.

REFERENCES

Barbuy B., 1994, ApJ, 430, 218

Beasley M. A., Hoyle F., Sharples R. M., 2002, MNRAS
Burstein D., Faber S. M., Gaskell C. M., Krumm N., 1984, ApJ, 287, 586
Carollo C. M., Danziger I. J., 1994, MNRAS, 270, 523
Cenarro A. J., Cardiel N., Gorgas J., Peletier R. F., Vazdekis A., Prada F., 2001, MNRAS, 326, 959
Davies R. L., Sadler E. M., Peletier R. F., 1993, MNRAS, 262, 650
de Freitas Pacheco J. A., Barbuy B., 1995, A&A, 302, 718
Eisenstein D. J., et al., 2003, ApJ, 585, 694
Faber S. M., Friel E. D., Burstein D., Gaskell D. M., 1985, ApJS, 57, 711
Fisher D., Franx M., Illingworth G., 1995, ApJ, 448, 119
Gehren T., 1975a, LTE-Sternatmosphärenmodelle (I), University of Kiel, Germany
Gehren T., 1975b, LTE-Sternatmosphärenmodelle (II), University of Kiel, Germany
Greggio L., 1997, MNRAS, 285, 151
Houdashelt M. L., Trager S. C., Worthey G., Bell R. A., 2002, Bulletin of the AAS, 34, 1118
Kuntschner H., 2000, MNRAS, 315, 184
Kuntschner H., Davies R. L., 1998, MNRAS, 295, L29
Kuntschner H., Ziegler B., Sharples R. M., Worthey G., Fricke K. J., 2002, A&A, 395, 761
Lee H., Yoon S., Lee Y., 2000, AJ, 120, 998
Maraston C., 1998, MNRAS, 300, 872
Maraston C., 2004, MNRAS, in preparation
Maraston C., Greggio L., Renzini A., Ortolani S., Saglia R. P., Puzia T., Kissler-Patig M., 2003, A&A, 400, 823
Maraston C., Thomas D., 2000, ApJ, 541, 126
Mehlert D., Thomas D., Saglia R. P., Bender R., Wegner G., 2003, A&A, 407, 423
Poggianti B., et al., 2001, ApJ, 562, 689
Puzia T., Saglia R. P., Kissler-Patig M., Maraston C., Greggio L., Renzini A., Ortolani S., 2002, A&A, 395, 45
Saglia R. P., Maraston C., Thomas D., Bender R., Colless M., 2002, ApJ, 579, L13
Sanchez-Blazquez P., Gorgas J., Cardiel N., Cenarro A. J., González J. J., 2003, ApJ, 509, L91
Surma P., Bender R., 1995, A&A, 298, 405
Terlevich A. I., Kuntschner H., Bower R. G., Caldwell N., Sharples R. M., 1999, MNRAS, 310, 445
Thomas D., Maraston C., Bender R., 2002, Ap&SS, 281, 371
Thomas D., Maraston C., Bender R., 2003a, MNRAS, 339, 897
Thomas D., Maraston C., Bender R., 2003b, MNRAS, 343, 279
Trager S. C., Faber S. M., Dressler A., 2004, AJ, in preparation
Trager S. C., Faber S. M., Worthey G., González J. J., 2000a, AJ, 119, 164
Trager S. C., Faber S. M., Worthey G., González J. J., 2000b, AJ, 120, 165
Tripicco M. J., Bell R. A., 1995, AJ, 110, 3035
Vazdekis A., Arimoto N., 1999, ApJ, 525, 144
Weiss A., Peletier R. F., Matteucci F., 1995, A&A, 296, 73
Worthey G., 1998, PASP, 110, 888
Worthey G., Faber S. M., González J. J., 1992, ApJ, 398, 69
Worthey G., Faber S. M., González J. J., Burstein D., 1994, ApJS, 94, 687
Worthey G., Ottaviani D. L., 1997, ApJS, 111, 377

This paper has been typeset from a TEX/ LATEX file prepared by the author.

Table A1. Simple stellar population models for the higher-order Balmer lines with $t = 1 – 15$ Gyr, $[Z/H] = −2.25 – 0.67$, and $[\alpha/Fe] = 0$.

Age (1)	[Z/H] (2)	[α/Fe] (3)	Hδ$_A$ (4)	Hδ$_F$ (5)	Hγ$_A$ (6)	Hγ$_F$ (7)	Age (1)	[Z/H] (2)	[α/Fe] (3)	Hδ$_A$ (4)	Hδ$_F$ (5)	Hγ$_A$ (6)	Hγ$_F$ (7)
1	−2.25	0.00	10.53	8.26	10.48	8.11	1	0.00	0.00	5.54	4.01	3.88	3.74
2	−2.25	0.00	8.38	6.29	7.70	6.06	2	0.00	0.00	1.09	1.72	−1.53	0.95
3	−2.25	0.00	8.07	5.90	6.88	5.50	3	0.00	0.00	−0.31	1.02	−3.35	0.00
4	−2.25	0.00	7.65	5.53	6.25	5.09	4	0.00	0.00	−0.81	0.76	−4.04	−0.37
5	−2.25	0.00	7.12	5.14	5.55	4.65	5	0.00	0.00	−1.29	0.53	−4.67	−0.71
6	−2.25	0.00	6.60	4.77	4.86	4.24	6	0.00	0.00	−1.70	0.34	−5.16	−0.98
7	−2.25	0.00	6.06	4.44	4.30	3.90	7	0.00	0.00	−1.91	0.24	−5.41	−1.12
8	−2.25	0.00	5.71	4.23	4.00	3.70	8	0.00	0.00	−2.06	0.17	−5.58	−1.23
9	−2.25	0.00	5.40	4.19	3.35	3.45	9	0.00	0.00	−2.32	0.06	−5.88	−1.39
10	−2.25	0.00	5.57	4.25	3.33	3.43	10	0.00	0.00	−2.51	−0.02	−6.08	−1.51
11	−2.25	0.00	5.77	4.38	3.63	3.56	11	0.00	0.00	−2.78	−0.13	−6.37	−1.67
12	−2.25	0.00	5.83	4.48	3.75	3.62	12	0.00	0.00	−3.01	−0.23	−6.59	−1.79
13	−2.25	0.00	5.61	4.35	3.60	3.48	13	0.00	0.00	−3.21	−0.31	−6.78	−1.90
14	−2.25	0.00	5.20	4.10	3.07	3.15	14	0.00	0.00	−3.40	−0.39	−6.96	−2.00
15	−2.25	0.00	4.97	3.94	2.86	2.98	15	0.00	0.00	−3.58	−0.46	−7.12	−2.09
1	−1.35	0.00	7.83	5.84	6.98	5.67	1	0.35	0.00	2.87	2.55	0.40	1.91
2	−1.35	0.00	7.44	5.41	6.40	5.24	2	0.35	0.00	−0.90	0.89	−3.93	−0.21
3	−1.35	0.00	6.72	4.89	5.36	4.64	3	0.35	0.00	−1.62	0.52	−4.87	−0.72
4	−1.35	0.00	5.79	4.29	4.15	3.96	4	0.35	0.00	−2.24	0.24	−5.63	−1.14
5	−1.35	0.00	4.88	3.73	2.94	3.29	5	0.35	0.00	−2.68	0.04	−6.14	−1.43
6	−1.35	0.00	4.19	3.30	2.05	2.78	6	0.35	0.00	−3.06	−0.13	−6.56	−1.66
7	−1.35	0.00	3.62	2.95	1.33	2.37	7	0.35	0.00	−3.28	−0.22	−6.78	−1.78
8	−1.35	0.00	3.29	2.75	0.93	2.13	8	0.35	0.00	−3.50	−0.31	−7.00	−1.92
9	−1.35	0.00	2.93	2.54	0.42	1.84	9	0.35	0.00	−3.70	−0.39	−7.19	−2.03
10	−1.35	0.00	2.75	2.40	0.17	1.68	10	0.35	0.00	−3.95	−0.49	−7.43	−2.16
11	−1.35	0.00	2.70	2.34	0.10	1.62	11	0.35	0.00	−4.21	−0.60	−7.67	−2.30
12	−1.35	0.00	2.79	2.32	0.27	1.63	12	0.35	0.00	−4.42	−0.69	−7.86	−2.41
13	−1.35	0.00	3.06	2.54	0.57	1.83	13	0.35	0.00	−4.60	−0.76	−8.03	−2.50
14	−1.35	0.00	3.76	3.01	1.36	2.27	14	0.35	0.00	−4.77	−0.84	−8.16	−2.58
15	−1.35	0.00	4.08	3.22	1.70	2.44	15	0.35	0.00	−4.94	−0.90	−8.30	−2.66
1	−0.33	0.00	5.52	4.11	3.95	3.84	1	0.67	0.00	1.83	2.14	−0.41	1.60
2	−0.33	0.00	2.62	2.52	0.35	1.95	2	0.67	0.00	−1.80	0.57	−4.85	−0.62
3	−0.33	0.00	1.47	1.90	−1.06	1.20	3	0.67	0.00	−3.34	−0.10	−6.67	−1.62
4	−0.33	0.00	0.79	1.50	−1.92	0.71	4	0.67	0.00	−4.18	−0.47	−7.58	−2.11
5	−0.33	0.00	0.40	1.28	−2.48	0.40	5	0.67	0.00	−4.44	−0.59	−7.84	−2.26
6	−0.33	0.00	0.08	1.10	−2.95	0.15	6	0.67	0.00	−4.62	−0.67	−8.02	−2.36
7	−0.33	0.00	−0.23	0.94	−3.36	−0.08	7	0.67	0.00	−4.83	−0.76	−8.22	−2.48
8	−0.33	0.00	−0.46	0.82	−3.67	−0.25	8	0.67	0.00	−5.06	−0.86	−8.44	−2.61
9	−0.33	0.00	−0.70	0.70	−3.99	−0.43	9	0.67	0.00	−5.34	−0.98	−8.70	−2.75
10	−0.33	0.00	−0.99	0.55	−4.35	−0.63	10	0.67	0.00	−5.66	−1.11	−8.99	−2.92
11	−0.33	0.00	−1.23	0.44	−4.65	−0.79	11	0.67	0.00	−5.79	−1.18	−9.10	−2.99
12	−0.33	0.00	−1.42	0.34	−4.87	−0.93	12	0.67	0.00	−5.93	−1.25	−9.22	−3.06
13	−0.33	0.00	−1.57	0.28	−5.05	−1.02	13	0.67	0.00	−6.06	−1.32	−9.33	−3.12
14	−0.33	0.00	−1.63	0.27	−5.11	−1.05	14	0.67	0.00	−6.15	−1.36	−9.40	−3.16
15	−0.33	0.00	−1.74	0.23	−5.25	−1.12	15	0.67	0.00	−6.22	−1.40	−9.46	−3.20

APPENDIX A: MODEL TABLES

Table A2. Simple stellar population models for the higher-order Balmer lines with $t = 1 - 15$ Gyr, $[Z/H] = -2.25 - 0.67$, and $[\alpha/Fe] = 0.3$.

Age (1)	$[Z/H]$ (2)	$[\alpha/Fe]$ (3)	$H\delta_A$ (4)	$H\delta_F$ (5)	$H\gamma_A$ (6)	$H\gamma_F$ (7)	Age (1)	$[Z/H]$ (2)	$[\alpha/Fe]$ (3)	$H\delta_A$ (4)	$H\delta_F$ (5)	$H\gamma_A$ (6)	$H\gamma_F$ (7)
1	−2.25	0.30	10.65	8.30	10.47	8.09	1	0.00	0.30	6.22	4.32	4.40	3.91
2	−2.25	0.30	8.50	6.33	7.70	6.05	2	0.00	0.30	1.94	2.10	−0.85	1.17
3	−2.25	0.30	8.18	5.94	6.88	5.48	3	0.00	0.30	0.71	1.46	−2.52	0.27
4	−2.25	0.30	7.77	5.58	6.24	5.07	4	0.00	0.30	0.23	1.21	−3.19	−0.10
5	−2.25	0.30	7.24	5.19	5.54	4.63	5	0.00	0.30	−0.22	0.99	−3.79	−0.43
6	−2.25	0.30	6.73	4.82	4.86	4.22	6	0.00	0.30	−0.58	0.81	−4.24	−0.69
7	−2.25	0.30	6.19	4.49	4.29	3.88	7	0.00	0.30	−0.79	0.72	−4.48	−0.83
8	−2.25	0.30	5.84	4.29	3.99	3.68	8	0.00	0.30	−0.92	0.65	−4.65	−0.94
9	−2.25	0.30	5.54	4.25	3.33	3.43	9	0.00	0.30	−1.16	0.55	−4.92	−1.09
10	−2.25	0.30	5.71	4.30	3.32	3.41	10	0.00	0.30	−1.32	0.48	−5.11	−1.21
11	−2.25	0.30	5.91	4.44	3.62	3.54	11	0.00	0.30	−1.55	0.38	−5.36	−1.35
12	−2.25	0.30	5.97	4.53	3.74	3.60	12	0.00	0.30	−1.73	0.30	−5.55	−1.47
13	−2.25	0.30	5.76	4.41	3.59	3.46	13	0.00	0.30	−1.89	0.23	−5.72	−1.57
14	−2.25	0.30	5.34	4.15	3.05	3.12	14	0.00	0.30	−2.03	0.17	−5.86	−1.66
15	−2.25	0.30	5.11	4.00	2.84	2.96	15	0.00	0.30	−2.17	0.11	−5.99	−1.75
1	−1.35	0.30	7.98	5.92	7.07	5.68	1	0.35	0.30	3.93	3.04	1.19	2.17
2	−1.35	0.30	7.60	5.49	6.49	5.24	2	0.35	0.30	0.42	1.48	−2.90	0.12
3	−1.35	0.30	6.88	4.98	5.46	4.65	3	0.35	0.30	−0.27	1.12	−3.83	−0.39
4	−1.35	0.30	5.97	4.39	4.25	3.97	4	0.35	0.30	−0.84	0.85	−4.54	−0.79
5	−1.35	0.30	5.08	3.83	3.05	3.30	5	0.35	0.30	−1.24	0.67	−5.01	−1.07
6	−1.35	0.30	4.39	3.41	2.17	2.80	6	0.35	0.30	−1.57	0.52	−5.39	−1.29
7	−1.35	0.30	3.84	3.06	1.46	2.38	7	0.35	0.30	−1.76	0.44	−5.60	−1.42
8	−1.35	0.30	3.51	2.86	1.07	2.15	8	0.35	0.30	−1.95	0.35	−5.80	−1.55
9	−1.35	0.30	3.17	2.66	0.56	1.86	9	0.35	0.30	−2.12	0.28	−5.97	−1.66
10	−1.35	0.30	3.00	2.52	0.32	1.70	10	0.35	0.30	−2.31	0.20	−6.17	−1.78
11	−1.35	0.30	2.94	2.47	0.26	1.64	11	0.35	0.30	−2.51	0.11	−6.37	−1.91
12	−1.35	0.30	3.05	2.44	0.43	1.65	12	0.35	0.30	−2.67	0.04	−6.52	−2.01
13	−1.35	0.30	3.32	2.67	0.73	1.85	13	0.35	0.30	−2.80	−0.01	−6.65	−2.09
14	−1.35	0.30	4.02	3.14	1.52	2.29	14	0.35	0.30	−2.91	−0.06	−6.75	−2.17
15	−1.35	0.30	4.34	3.34	1.86	2.46	15	0.35	0.30	−3.01	−0.11	−6.84	−2.23
1	−0.33	0.30	6.14	4.37	4.32	3.95	1	0.67	0.30	3.03	2.66	0.33	1.83
2	−0.33	0.30	3.33	2.82	0.77	2.09	2	0.67	0.30	−0.41	1.17	−3.96	−0.35
3	−0.33	0.30	2.21	2.21	−0.62	1.34	3	0.67	0.30	−1.77	0.56	−5.64	−1.31
4	−0.33	0.30	1.56	1.82	−1.45	0.86	4	0.67	0.30	−2.47	0.24	−6.43	−1.78
5	−0.33	0.30	1.18	1.60	−2.01	0.55	5	0.67	0.30	−2.69	0.13	−6.68	−1.92
6	−0.33	0.30	0.87	1.43	−2.46	0.30	6	0.67	0.30	−2.83	0.07	−6.83	−2.02
7	−0.33	0.30	0.59	1.28	−2.85	0.07	7	0.67	0.30	−2.99	0.00	−6.99	−2.14
8	−0.33	0.30	0.37	1.16	−3.16	−0.10	8	0.67	0.30	−3.17	−0.09	−7.18	−2.26
9	−0.33	0.30	0.15	1.05	−3.46	−0.27	9	0.67	0.30	−3.37	−0.18	−7.39	−2.40
10	−0.33	0.30	−0.12	0.91	−3.80	−0.47	10	0.67	0.30	−3.62	−0.29	−7.63	−2.56
11	−0.33	0.30	−0.33	0.80	−4.07	−0.62	11	0.67	0.30	−3.69	−0.34	−7.71	−2.62
12	−0.33	0.30	−0.49	0.71	−4.27	−0.75	12	0.67	0.30	−3.78	−0.40	−7.79	−2.68
13	−0.33	0.30	−0.62	0.66	−4.43	−0.83	13	0.67	0.30	−3.84	−0.44	−7.86	−2.74
14	−0.33	0.30	−0.65	0.66	−4.48	−0.86	14	0.67	0.30	−3.87	−0.47	−7.89	−2.78
15	−0.33	0.30	−0.74	0.63	−4.59	−0.93	15	0.67	0.30	−3.89	−0.49	−7.91	−2.81

Table A3. Simple stellar population models for the higher-order Balmer lines with $t = 1 - 15$ Gyr, $[Z/H] = -2.25 - 0.67$, and $[\alpha/Fe] = 0.5$.

Age (1)	$[Z/H]$ (2)	$[\alpha/Fe]$ (3)	$H\delta_A$ (4)	$H\delta_F$ (5)	$H\gamma_A$ (6)	$H\gamma_F$ (7)	Age (1)	$[Z/H]$ (2)	$[\alpha/Fe]$ (3)	$H\delta_A$ (4)	$H\delta_F$ (5)	$H\gamma_A$ (6)	$H\gamma_F$ (7)
1	−2.25	0.50	10.74	8.33	10.46	8.08	1	0.00	0.50	6.66	4.52	4.74	4.02
2	−2.25	0.50	8.57	6.36	7.70	6.04	2	0.00	0.50	2.50	2.35	−0.41	1.31
3	−2.25	0.50	8.26	5.97	6.87	5.47	3	0.00	0.50	1.37	1.75	−1.97	0.44
4	−2.25	0.50	7.85	5.61	6.24	5.06	4	0.00	0.50	0.90	1.50	−2.63	0.08
5	−2.25	0.50	7.33	5.22	5.54	4.62	5	0.00	0.50	0.49	1.29	−3.20	−0.25
6	−2.25	0.50	6.82	4.85	4.85	4.21	6	0.00	0.50	0.14	1.12	−3.64	−0.50
7	−2.25	0.50	6.28	4.53	4.28	3.87	7	0.00	0.50	−0.05	1.03	−3.87	−0.64
8	−2.25	0.50	5.94	4.33	3.98	3.66	8	0.00	0.50	−0.19	0.97	−4.04	−0.75
9	−2.25	0.50	5.64	4.29	3.33	3.42	9	0.00	0.50	−0.40	0.87	−4.29	−0.90
10	−2.25	0.50	5.81	4.34	3.31	3.39	10	0.00	0.50	−0.55	0.80	−4.47	−1.01
11	−2.25	0.50	6.01	4.48	3.61	3.53	11	0.00	0.50	−0.75	0.71	−4.70	−1.15
12	−2.25	0.50	6.07	4.57	3.73	3.59	12	0.00	0.50	−0.90	0.65	−4.87	−1.26
13	−2.25	0.50	5.86	4.45	3.58	3.44	13	0.00	0.50	−1.03	0.59	−5.02	−1.36
14	−2.25	0.50	5.44	4.19	3.04	3.11	14	0.00	0.50	−1.14	0.53	−5.14	−1.44
15	−2.25	0.50	5.21	4.04	2.83	2.94	15	0.00	0.50	−1.25	0.48	−5.25	−1.52
1	−1.35	0.50	8.08	5.97	7.13	5.68	1	0.35	0.50	4.62	3.35	1.71	2.34
2	−1.35	0.50	7.70	5.55	6.56	5.25	2	0.35	0.50	1.28	1.87	−2.23	0.33
3	−1.35	0.50	6.99	5.04	5.53	4.65	3	0.35	0.50	0.60	1.51	−3.14	−0.17
4	−1.35	0.50	6.09	4.45	4.33	3.98	4	0.35	0.50	0.07	1.26	−3.82	−0.57
5	−1.35	0.50	5.21	3.89	3.13	3.30	5	0.35	0.50	−0.31	1.08	−4.28	−0.84
6	−1.35	0.50	4.53	3.48	2.26	2.80	6	0.35	0.50	−0.60	0.94	−4.63	−1.05
7	−1.35	0.50	3.98	3.13	1.55	2.39	7	0.35	0.50	−0.78	0.86	−4.83	−1.18
8	−1.35	0.50	3.66	2.94	1.16	2.16	8	0.35	0.50	−0.95	0.79	−5.02	−1.31
9	−1.35	0.50	3.32	2.74	0.66	1.87	9	0.35	0.50	−1.10	0.72	−5.18	−1.41
10	−1.35	0.50	3.16	2.60	0.42	1.71	10	0.35	0.50	−1.26	0.65	−5.35	−1.54
11	−1.35	0.50	3.11	2.55	0.36	1.65	11	0.35	0.50	−1.42	0.58	−5.53	−1.66
12	−1.35	0.50	3.22	2.53	0.54	1.66	12	0.35	0.50	−1.55	0.52	−5.65	−1.75
13	−1.35	0.50	3.49	2.76	0.84	1.86	13	0.35	0.50	−1.64	0.48	−5.76	−1.83
14	−1.35	0.50	4.19	3.22	1.63	2.30	14	0.35	0.50	−1.71	0.44	−5.83	−1.90
15	−1.35	0.50	4.51	3.43	1.97	2.47	15	0.35	0.50	−1.78	0.41	−5.89	−1.96
1	−0.33	0.50	6.55	4.55	4.55	4.02	1	0.67	0.50	3.82	3.02	0.81	1.98
2	−0.33	0.50	3.80	3.01	1.05	2.17	2	0.67	0.50	0.50	1.56	−3.37	−0.17
3	−0.33	0.50	2.69	2.41	−0.33	1.42	3	0.67	0.50	−0.74	1.00	−4.96	−1.11
4	−0.33	0.50	2.06	2.03	−1.15	0.95	4	0.67	0.50	−1.36	0.71	−5.68	−1.57
5	−0.33	0.50	1.69	1.82	−1.69	0.64	5	0.67	0.50	−1.56	0.61	−5.92	−1.71
6	−0.33	0.50	1.39	1.65	−2.14	0.39	6	0.67	0.50	−1.67	0.55	−6.05	−1.81
7	−0.33	0.50	1.12	1.50	−2.52	0.17	7	0.67	0.50	−1.80	0.49	−6.19	−1.91
8	−0.33	0.50	0.91	1.39	−2.82	0.00	8	0.67	0.50	−1.94	0.42	−6.35	−2.03
9	−0.33	0.50	0.70	1.28	−3.11	−0.18	9	0.67	0.50	−2.11	0.34	−6.53	−2.17
10	−0.33	0.50	0.45	1.14	−3.43	−0.37	10	0.67	0.50	−2.30	0.24	−6.74	−2.32
11	−0.33	0.50	0.25	1.04	−3.70	−0.52	11	0.67	0.50	−2.35	0.20	−6.80	−2.38
12	−0.33	0.50	0.11	0.96	−3.88	−0.64	12	0.67	0.50	−2.40	0.16	−6.86	−2.44
13	−0.33	0.50	0.00	0.92	−4.03	−0.72	13	0.67	0.50	−2.42	0.13	−6.90	−2.49
14	−0.33	0.50	−0.01	0.92	−4.06	−0.74	14	0.67	0.50	−2.41	0.11	−6.91	−2.53
15	−0.33	0.50	−0.09	0.89	−4.16	−0.80	15	0.67	0.50	−2.39	0.11	−6.90	−2.55